15th Triennial World Congress, Barcelona, Spain

A FLEXIBLE-LINK AS AN ENDPOINT POSITION AND FORCE DETECTION UNIT

Min Gu and Jean-Claude Piedboeuf

Space Technologies, Canadian Space Agency
6767 route de l'Aéroport, St-Hubert
Québec, Canada
email: Jean-Claude.Piedboeuf@space.gc.ca

Abstract: A flexible robot arm with strain gauges distributed on it is used as a sensing unit in determination of endpoint position and force of flexible manipulator. The position and orientation of the flexible arm is expressed as a function of the local curvature. An interpolation technique gave a continuous curvature function from a finite set of measurements made with strain gauges. The endpoint force and moment depend not only on the local strains but also on the positions and orientations of the endpoint and those points where the strain gauges are located. Using the measured strains, one obtained the endpoint position and orientation as well as force and moment of the flexible arm. The experimental results demonstrated the effectiveness and accuracy of the proposed approach.

Keywords: Flexible arm, Endpoint, Position, Force, Detection algorithms, Tests.

1. INTRODUCTION

Precise position and force control is required for many applications in space robotics, including assembly and on-orbit service of international space station. To achieve precise position and force control, an accurate determination of the endpoint position and force is required. In a rigid robot, the endpoint position and force can be determined using the joint position sensors and a force sensor at the end-effector. However, this is not the case for a flexible space manipulator. The endpoint of a flexible manipulator depends not only on the joint positions but also on the deformations of its flexible links. The variation of the endpoint position and orientation due to link deformations also results in an error in the transformation of the endpoint force and moment in the joint space.

Because flexible manipulators are distributed systems and have infinite degrees of freedom, it is impossible to use the collocated sensors like rigid manipulator to detect all degrees of freedom. Up to date, vision systems have been used to detect the endpoint position of planar flexible manipulators (Cannon and Schmitz, 1984; Oakley, 1991). This kind of systems directly detects the manipulator's endpoint and has the advantage to be compatible with any robot. However, the vision system usually has limited view range. Obstructions and interference result in lost information. Integration of external vision system into a robotic manipulator could be a problem. Low sampling rate also limits its application in tri-dimensional motion and dynamic control.

To overcome the limitation of vision system, strain gauge method has been proposed (Piedboeuf and Miller, 1994). In this method, a finite set of local strains detected by the strain gauges is used to construct the continuous functions of the curvatures along the flexible link. The endpoint position and orientation can be determined from the integration of these curvature functions. Strain gauge method requires only a kinematic model of flexible link and simple matrix calculations, and has been shown to be effective and accurate in both static and dynamic cases (Gu and Piedboeuf, 2001). The detailed derivation and verification of nonlinear kinematic model for flexible beam element can be found in a technical report (Gu, 2001*b*).

With the exception of position detection, strain gauge has also been used to detect the endpoint force of flexible manipulator (Richter and Pfeiffer, 1991; Kim *et al.*, 1996). However, the previous studies used only one strain gauge location at the root of each link and employed a simplified model to determine the endpoint force. Actually, the flexible link in a space flexible manipulator can encounter very complicated loading situations and exhibit complex deformation configuration. Using only one strain gauge location cannot obtain enough information and provide accurate measurement of the endpoint force and moment. In this paper, the strain gauges are placed at the four positions of each flexible link and detect both bending and torsion strains at the each position. These four sets of strain measurements are then used to determine the endpoint position and force of the flexible link. One can determine the endpoint position and force of a flexible manipulator by considering the kinematics and statics of both rigid and flexible links. Because the positions and orientations of flexible links are considered in the force transformation, accurate endpoint force and moment are obtained. The experimental results demonstrated the effectiveness and accuracy of the proposed approach.

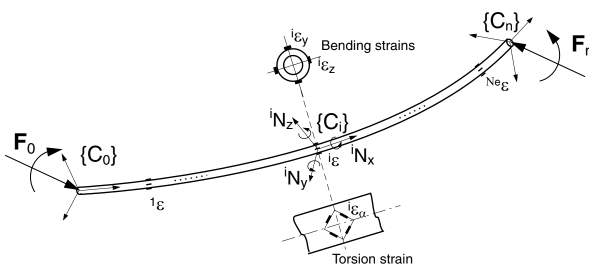

Fig. 1. Flexible link unit and force detection

2. FLEXIBLE LINK UNIT

A cylindrical flexible link used as a position and force measurement unit is shown in Fig. 1. There are N_e positions where the strain gauges are located. In each position, the strain gauges detect two bending strains (ϵ_y, ϵ_z) and one torsion strain (ϵ_α). The measured bending and torsion strains can be expressed as N_e local strain vectors:

$$ {}^i\boldsymbol{\epsilon} = \begin{bmatrix} {}^i\epsilon_\alpha \\ {}^i\epsilon_y \\ {}^i\epsilon_z \end{bmatrix} \quad i = 1, 2, \cdots, N_e \tag{1} $$

These strain vectors provide the basic information of the link deformations. It is our purpose to use this information to determine the endpoint position and orientation as well as endpoint force and moment of the flexible link. To achieve this purpose, the relations between the local strains and the curvatures as well as the internal forces of link sections are determined. According to the beam bending and torsion theory, the curvatures of a flexible link is proportional to the strain vector as:

$$ {}^i\boldsymbol{\kappa} = \mathbf{C}_a \, {}^i\boldsymbol{\epsilon} \quad i = 1, 2, \cdots, N_e \tag{2} $$

where

$$ {}^i\boldsymbol{\kappa} = \begin{bmatrix} {}^i\kappa_x \\ {}^i\kappa_y \\ {}^i\kappa_z \end{bmatrix} \quad \mathbf{C}_a = \begin{bmatrix} 1/c_\alpha & 0 & 0 \\ 0 & 1/c_y & 0 \\ 0 & 0 & 1/c_z \end{bmatrix} \tag{3} $$

The constants c_α, c_y and c_z in Eq. 3 are the active radius that depends on the distance from the neutral axis of the link to the associated strain gauges. For a cylindrical flexible beam with outside diameter of D_o, this radius is $D_0/2$.

The internal forces associated with the strain measurements include two bending moments and a torsion torque, and are expressed as:

$$ {}^i\mathbf{N} = \begin{bmatrix} {}^iN_x \\ {}^iN_y \\ {}^iN_z \end{bmatrix} \quad i = 1, 2, \cdots, N_e \tag{4} $$

A proportional relation between the moment vector ${}^i\mathbf{N}$ and the local strain vector ${}^i\boldsymbol{\epsilon}$ can be found as:

$$ {}^i\mathbf{N} = \mathbf{C}_e \, {}^i\boldsymbol{\epsilon} \quad i = 1, 2, \cdots, N_e \tag{5} $$

where the strain-to-force gains are given by

$$ \mathbf{C}_e = \begin{bmatrix} \dfrac{GI_x}{c_\alpha} & 0 & 0 \\ 0 & \dfrac{EI_z}{c_y} & 0 \\ 0 & 0 & \dfrac{EI_y}{c_z} \end{bmatrix} \tag{6} $$

EI_z, EI_y and GI_x represent the bending and torsion stiffness of the link cross section.

3. POSE DETERMINATION

To determine the position and orientation of a flexible link, a moving local frame $\{C_i\}$ is defined along the link as shown in Fig. 1. The moving frame has its x axis tangent to the neutral axis and can move along the neutral axis. At any instant, the position and orientation of the moving frame are a function of the space variable s, which represents the arc length of the neutral axis measured from the base point of the link to an any given point at the neutral axis. When $s = 0$, the moving frame is located at the base point and called as the base frame $\{C_0\}$. When $s = L$, the moving frame is located at the end point and called as the endpoint frame $\{C_n\}$.

The position and orientation of a flexible link has a one-to-one relation with the curvature of the link. Recalling the kinematics developed by Piedboeuf (Piedboeuf, 1995), the rotation matrix and position vector mapping the frame $\{C_i\}$ to frame $\{C_0\}$ are expressed as:

$$
{}^0_i\mathbf{R}=\begin{bmatrix} 1-\frac{1}{2}(v'^2+w'^2) & -v'-\int_0^s \alpha' w' d\xi & -w'+\int_0^s \alpha' v' d\xi \\ v'-\int_0^s \alpha w'' d\xi & 1-\frac{1}{2}(v'^2+\alpha^2) & -\alpha-\int_0^s v' w'' d\xi \\ w'+\int_0^s \alpha v'' d\xi & \alpha-\int_0^s v'' w' d\xi & 1-\frac{1}{2}(w'^2+\alpha^2) \end{bmatrix} \quad (7)
$$

$$
{}^0\mathbf{p}_i = \begin{bmatrix} p_x \\ p_y \\ p_z \end{bmatrix} = \begin{bmatrix} s-\frac{1}{2}\int_0^s (v'^2+w'^2) d\xi \\ v-\int_0^s \int_0^\xi w'' \alpha d\eta d\xi \\ w+\int_0^s \int_0^\xi v'' \alpha d\eta d\xi \end{bmatrix} \quad (8)
$$

where w, v, and α represent the deflections and torsion angle of the flexible link respectively and are defined by:

$$
v=\int_0^s \int_0^\xi {}^i\kappa_z d\eta d\xi \quad w=-\int_0^s \int_0^\xi {}^i\kappa_y d\eta d\xi \quad \alpha=\int_0^s {}^i\kappa_x d\xi \quad (9)
$$

Using Eq. 7 and Eq. 8, one can obtain the endpoint position and orientation as long as the curvatures ${}^i\kappa_x$,${}^i\kappa_y$ and ${}^i\kappa_z$ are known. However, a practical problem is that only a finite number of strain gauges can be used while a continuous function for the curvature is required. Therefore we must use interpolation technique to reconstruct the curvature along the link. Piedboeuf and Miller (Piedboeuf and Miller, 1994) have developed an interpolation algorithm using the polynomial function. The algorithm considered only the first order term of the endpoint position and orientation. In order to show the coupling between the bending and torsion, the second order term in Eq. 7 and Eq. 8 must be included. Using the same approach as Piedboeuf and Miller (Piedboeuf and Miller, 1994), we obtain the algorithm that determine the endpoint position and orientation up to the second order:

$$
{}^0\mathbf{p}_n = \mathbf{P}_1 + \mathbf{P}_2 \quad (10)
$$

$$
{}^0_n\mathbf{R} = \mathbf{R}_1 + \mathbf{R}_2 \quad (11)
$$

$\mathbf{P}_1$ and $\mathbf{R}_1$ represent the first order terms and $\mathbf{P}_2$ and $\mathbf{R}_2$ represent the second order terms. They are defined as follows:

$$
\mathbf{P}_1 = \begin{bmatrix} 0 \\ \mathbf{a}_z^T \mathbf{II}_z \\ -\mathbf{a}_y^T \mathbf{II}_y \end{bmatrix} \quad (12)
$$

$$
\mathbf{R}_1 = \begin{bmatrix} 1 & -\mathbf{a}_z^T\mathbf{I}_z & \mathbf{a}_y^T\mathbf{I}_y \\ \mathbf{a}_z^T\mathbf{I}_z & 1 & -\mathbf{a}_x^T\mathbf{I}_x \\ -\mathbf{a}_y^T\mathbf{I}_y & \mathbf{a}_x^T\mathbf{I}_x & 1 \end{bmatrix} \quad (13)
$$

$$
\mathbf{P}_2 = \begin{bmatrix} -\frac{1}{2}(\mathbf{a}_y^T\mathbf{II}_y^2\mathbf{a}_y+\mathbf{a}_z^T\mathbf{II}_z^2\mathbf{a}_z) \\ \mathbf{a}_x^T\mathbf{III}_{xy}\mathbf{a}_y \\ \mathbf{a}_x^T\mathbf{III}_{xz}\mathbf{a}_z \end{bmatrix} \quad (14)
$$

$$
\mathbf{R}_2=\begin{bmatrix} -\frac{1}{2}(\mathbf{a}_y^T\mathbf{I}_y^2\mathbf{a}_y+\mathbf{a}_z^T\mathbf{I}_z^2\mathbf{a}_z) & \mathbf{a}_y^T\mathbf{II}_{yx}\mathbf{a}_x & \mathbf{a}_z^T\mathbf{II}_{zx}\mathbf{a}_x \\ \mathbf{a}_x^T\mathbf{II}_{xy}\mathbf{a}_y & -\frac{1}{2}(\mathbf{a}_z^T\mathbf{I}_z^2\mathbf{a}_z+\mathbf{a}_x^T\mathbf{I}_x^2\mathbf{a}_x) & \mathbf{a}_z^T\mathbf{II}_{zy}\mathbf{a}_y \\ \mathbf{a}_x^T\mathbf{II}_{xz}\mathbf{a}_z & \mathbf{a}_y^T\mathbf{II}_{yz}\mathbf{a}_z & -\frac{1}{2}(\mathbf{a}_x^T\mathbf{I}_x^2\mathbf{a}_x+\mathbf{a}_y^T\mathbf{I}_y^2\mathbf{a}_y) \end{bmatrix} \quad (15)
$$

$\mathbf{a}_k(k = x, y, z)$ represents the polynomial coefficients and are determined from the curvature $\boldsymbol{\kappa}_k(k = x, y, z)$ and the position matrix $\mathbf{S}$ of the strain gauges:

$$
\mathbf{a}_k = (\mathbf{S}^T\mathbf{S})^{-1}\mathbf{S}^T\boldsymbol{\kappa}_k \qquad k = x, y, z \quad (16)
$$

$$
\mathbf{S} = \begin{bmatrix} 1 & s_1 & s_1^2 & \cdots & s_1^{n_k} \\ 1 & s_2 & s_2^2 & \cdots & s_2^{n_k} \\ \vdots & \vdots & \vdots & \vdots & \vdots \\ 1 & s_{N_e} & s_{N_e}^2 & \cdots & s_{N_e}^{n_k} \end{bmatrix} \; N_e \geq n_k + 1 \quad (17)
$$

where n_k is the order of the polynomial. It has been shown that the polynomial order 2 is enough for a good fitting (Gu and Piedboeuf, 2001). The position integration vectors and matrices are defined as follows:

$$
\mathbf{I}_k = \begin{bmatrix} \vdots \\ L^i/i \\ \vdots \end{bmatrix} \qquad \begin{matrix} k = x, y, z \\ i = 1, \cdots, n_k + 1 \end{matrix} \quad (18)
$$

$$
\mathbf{II}_k = \begin{bmatrix} \vdots \\ L^{i+1}/(i^2+i) \\ \vdots \end{bmatrix} \qquad \begin{matrix} k = y, z \\ i = 1, \cdots, n_k + 1 \end{matrix} \quad (19)
$$

$$
\mathbf{I}_k^2 = \begin{bmatrix} \ddots & & \\ & \frac{L^{i+j}}{i \times j} & \\ & & \ddots \end{bmatrix} \qquad \begin{matrix} k = y, z \\ i, j = 1, \cdots, n_k + 1 \end{matrix} \quad (20)
$$

$$
\mathbf{II}_k^2 = \begin{bmatrix} \ddots & & \\ & \frac{L^{i+j+1}}{i \times j \times (i+j+1)} & \\ & & \ddots \end{bmatrix} \qquad \begin{matrix} k=y,z \\ i,j=1,\cdots,n_k+1 \end{matrix} \quad (21)
$$

$$
\mathbf{II}_{k_1k_2} = \begin{bmatrix} \ddots & & \\ & \frac{L^{i+j}}{i \times (i+j)} & \\ & & \ddots \end{bmatrix} \qquad \begin{matrix} k_1,k_2=x,y,z \\ k_1 \neq k_2 \\ i=1,\cdots,N_{k_1}+1 \\ j=1,\cdots,N_{k_2}+1 \end{matrix} \quad (22)
$$

$$
\mathbf{III}_{xk} = \begin{bmatrix} \ddots & & \\ & \frac{L^{i+j+1}}{i \times (i+j) \times (i+j+1)} & \\ & & \ddots \end{bmatrix} \qquad \begin{matrix} k=y,z \\ i=1,\cdots,N_x+1 \\ j=1,\cdots,N_k+1 \end{matrix} \quad (23)
$$

Determination of endpoint position and orientation is straightforward using Eq. 10 - Eq. 23, which involves only simple matrix computation. The position and orientation of any point (frame $\{C_i\}$) on the flexible link can be determined by replacing L with s_i, the arc length from frame $\{C_0\}$ to $\{C_i\}$.

4. STATICS

The external forces are considered to apply at the both ends of the flexible link as shown in Fig. 1, where ${}^n\mathbf{F}_n$ denotes the force applied at the endpoint of the link and ${}^0\mathbf{F}_0$ represents the reaction force at the base point of the link. For convenience, the forces are expressed in the local frames, and $\{C_i\}$ is located at the ith strain gauge position.

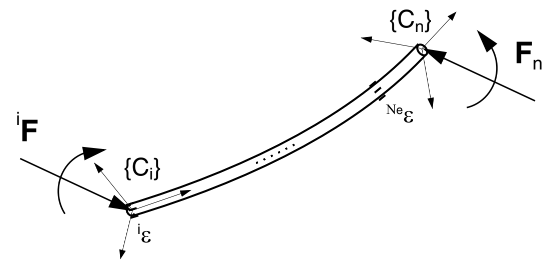

Fig. 2. Force balance for a flexible beam section

When cutting the flexible link into two sections at the frame $\{C_i\}$, an internal force ${}^i\mathbf{F}$ is used to balance the cutting section as shown in Fig. 2. Summing the forces and moments and setting them equal to zero results in:

$$ {}^i\mathbf{F} = {}^i_n\mathbf{T}_f \; {}^n\mathbf{F}_n \tag{24} $$

with

$$ {}^i\mathbf{F} = \begin{bmatrix} {}^i\mathbf{V} \\ {}^i\mathbf{N} \end{bmatrix} \quad {}^n\mathbf{F}_n = \begin{bmatrix} {}^n\mathbf{f}_n \\ {}^n\mathbf{n}_n \end{bmatrix} \tag{25} $$

$$ {}^i_n\mathbf{T}_F = \begin{bmatrix} {}^i_n\mathbf{R} & 0 \\ {}^i\mathbf{p}_n \times {}^i_n\mathbf{R} & {}^i_n\mathbf{R} \end{bmatrix} \tag{26} $$

where ${}^i\mathbf{p}_n$ and ${}^i_n\mathbf{R}$ represent the position and orientation of the endpoint frame $\{C_n\}$ relative to the frame $\{C_i\}$. For simplicity, the gravity of the flexible link is not considered in the above formulation. The internal force ${}^i\mathbf{F}$ consists of a force vector ${}^i\mathbf{V}$ and a moment vector ${}^i\mathbf{N}$. Because the strain gauges detect only the bending and torsion strains, the internal moment vector is the available portion in Eq. 24 and one can write the following equation:

$$ {}^i\mathbf{N} = \left[{}^i\mathbf{p}_n \times {}^i_n\mathbf{R} \;\; {}^i_n\mathbf{R} \right] \; {}^n\mathbf{F}_n \quad i = 1, 2, \cdots, N_e \tag{27} $$

Substituting the strain-force relation given in Eq. 5, we obtain a linear relation between the endpoint force and the measured strains as:

$$ \Delta\boldsymbol{\epsilon} = \mathbf{C}_n \; {}^n\mathbf{F}_n \tag{28} $$

where

$$ \Delta\boldsymbol{\epsilon} = \left[\Delta^1\boldsymbol{\epsilon} \; \cdots \; \Delta^i\boldsymbol{\epsilon} \; \cdots \; \Delta^{N_e}\boldsymbol{\epsilon} \right]^T \tag{29} $$

$$ \mathbf{C}_n = \begin{bmatrix} \mathbf{C}_e^{-1} \; {}^1\mathbf{p}_n \times {}^1_n\mathbf{R} & \mathbf{C}_e^{-1} \; {}^1_n\mathbf{R} \\ \vdots & \vdots \\ \mathbf{C}_e^{-1} \; {}^i\mathbf{p}_n \times {}^i_n\mathbf{R} & \mathbf{C}_e^{-1} \; {}^i_n\mathbf{R} \\ \vdots & \vdots \\ \mathbf{C}_e^{-1} \; {}^{N_e}\mathbf{p}_n \times {}^{N_e}_n\mathbf{R} & \mathbf{C}_e^{-1} \; {}^{N_e}_n\mathbf{R} \end{bmatrix} \tag{30} $$

$\Delta\boldsymbol{\epsilon}$ denotes the change of the strains caused by the endpoint force ${}^n\mathbf{F}_n$. The actual measured strain $\boldsymbol{\epsilon}$ also includes the strains caused by the gravity of the flexible link itself. ${}^i\mathbf{p}_n$ and ${}^i_n\mathbf{R}$ can be determined using the following formulation:

$$ {}^i\mathbf{p}_n = {}^0_i\mathbf{R}^T({}^0\mathbf{p}_n - {}^0\mathbf{p}_i) \tag{31} $$

$$ {}^i_n\mathbf{R} = {}^0_i\mathbf{R}^T \; {}^0_n\mathbf{R} \tag{32} $$

Using Eq. 28, the endpoint force can be expressed as a function of the measurement strains:

$$ {}^n\mathbf{F}_n = {}^n\mathbf{C}_F \; \Delta\boldsymbol{\epsilon} \tag{33} $$

where the force measurement matrix ${}^n\mathbf{C}_F$ is given by:

$$ {}^n\mathbf{C}_F = (\mathbf{C}_n^T \; \mathbf{C}_n)^{-1} \; \mathbf{C}_n^T \tag{34} $$

Eq. 33 gives the endpoint force and moment that are expressed in the endpoint frame $\{C_n\}$. The endpoint frame is a local frame and its position and orientation vary as the endpoint position and orientation change. In some cases, it is required to know the endpoint force that is expressed in the base frame $\{C_0\}$ of the flexible link. This endpoint force may be denoted by ${}^0\mathbf{F}_n$. Using rotation matrix ${}^0_n\mathbf{R}$, the endpoint force ${}^n\mathbf{F}_n$ can be transform to the base frame $\{C_0\}$ and the endpoint force ${}^0\mathbf{F}_n$ is expressed as:

$$ {}^0\mathbf{F}_n = {}^0_n\mathbf{R} \; {}^n\mathbf{F}_n \tag{35} $$

It is clear that the determination of the endpoint force and moment of a flexible link requires the knowledge of the positions and orientations of the endpoint as well as those points where the strain gauges are located.

5. VALIDATION

The use of strain gauges to obtain the endpoint position and force is especially useful for the flexible manipulator implementing a hybrid position and force control. This is the case of a space flexible manipulator performing a complex operation such as assembly of a component for the space station. Under this situation, the flexible link usually undergoes both bending and torsion deformations. To validate our approach, the position and force tests were conducted on a flexible link as shown in Fig. 3. The flexible link is a cylindrical beam of 1.4 meters long and has the strain gauges located at the four positions. In each position, the strain gauges detect the two bending strains and a torsion strain. Using these four sets of strain measurements, the endpoint position and force were then determined using the algorithms developed in Section 3 and Section 4.

Experimentally, the flexible beam was held at its base by a six degrees of freedom rigid robot. An external

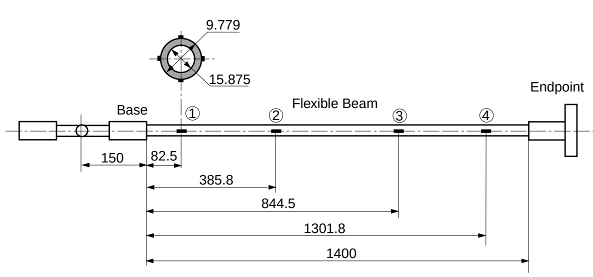

Fig. 3. Flexible beam using for the validation

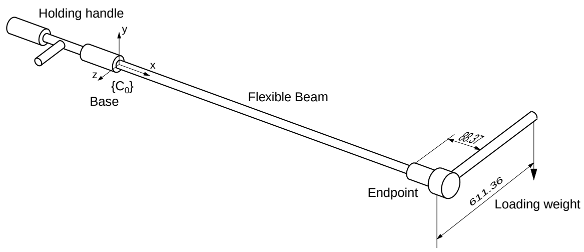

Fig. 4. Loading configuration in the static tests

force was applied to the endpoint of the flexible beam by hanging a weight at the end of an extension bar that is fixed to the endpoint of the beam as shown in Fig. 4. The loading configuration mainly results in a vertical force, a bending moment and a torsion torque acting on the endpoint of the flexible link.

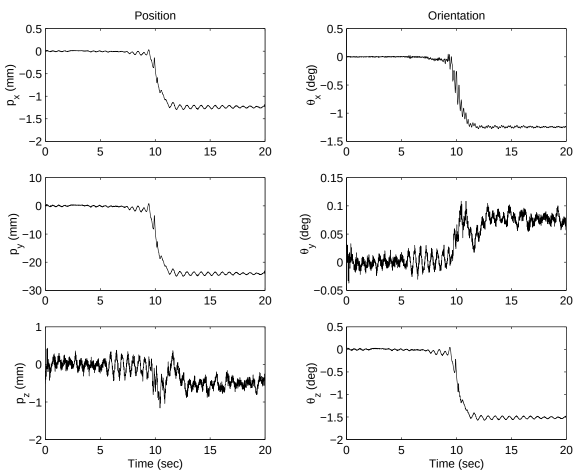

Fig. 5. Endpoint responses under static load 1.357 kg

Two weights, one is 1.357 kg and the other is 2.273 kg, have been used in the tests. Fig. 5 shows the response of the endpoint position and orientation obtained from the strain gauges when a loading weight of 1.357 kg is applied. In order to show the endpoint position and orientation caused by the loading weight only, the endpoint position and orientation in the plots are set to zeros when the load is not applied to the link. The actual endpoint position and orientation may be different because of the gravity of the flexible link. The orientation is represented using the Euler angles that are obtained from the rotation matrix (Gu and Piedboeuf, 2001). Because the load is applied in the vertical direction, large endpoint deflection appears in y direction and p_y is about 25 mm. The corresponding endpoint orientation is about 1.5 degrees. However, due to the coupling of torsion and bending there is a small deflection in the horizontal direction (z axis) and a small rotation about y axis. This can be explained from Eq. 7 and Eq. 8, in which the coupling second order terms in p_z and θ_y depend on the torsion about x-axis and the bending in y direction. It can be seen in Fig. 5 that the corresponding p_z is about 1 mm and θ_y is about 0.08 degrees. The foreshortening of the beam, p_x is caused by the beam bending and is about 1.4 mm, which is well detected by the strain gauges.

The endpoint orientation, θ_x is mainly caused by the torsion of the beam, and have a value of 1.25 degrees. The detection results in Fig. 5 has been shown to be compatible to the one obtained using the Optotrak vision system (Gu and Piedboeuf, 2001).

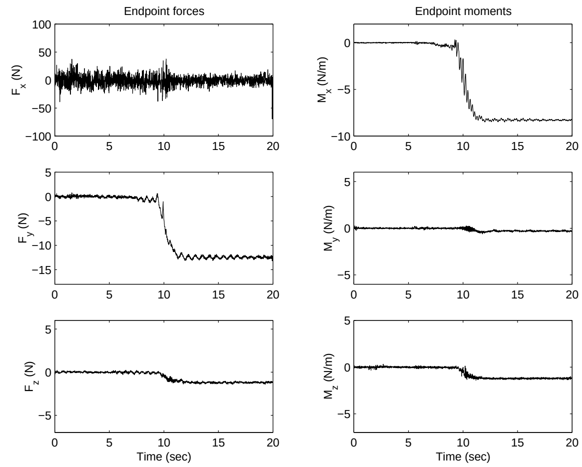

Fig. 6. ${}^{n}\mathbf{F}_n$ caused by static load 1.357 kg

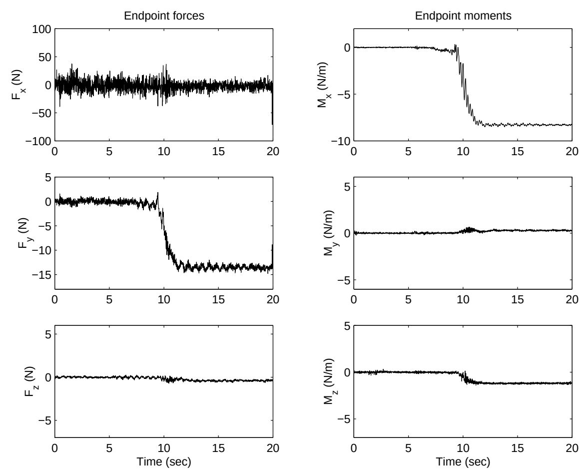

Fig. 7. ${}^{0}\mathbf{F}_n$ caused by static load 1.357 kg

Fig. 6 and Fig. 7 shows the response of the endpoint forces and moment when the loading weight 1.357 kg is applied. It is noticed that ${}^{n}\mathbf{F}_n$ and ${}^{0}\mathbf{F}_n$ are the same endpoint force but are expressed in the different frames. ${}^{n}\mathbf{F}_n$ is expressed in the endpoint frame $\{C_n\}$, which varies as the endpoint position and orientation change. ${}^{0}\mathbf{F}_n$ is expressed in the base frame $\{C_0\}$ of the flexible link, which is fixed during the tests. This frame coincides with the inertial frame and its negative y axis is the gravitational direction as shown in Fig. 4.

In Fig. 7, the major responses appear in F_y and M_x and a small response appears in M_z, which are what we expected from the loading configuration. In Fig. 6, there are small responses in F_z and M_y. This is because the endpoint force ${}^{n}\mathbf{F}_n$ is expressed in the endpoint frame $\{C_n\}$, which is not coincident with the inertial frame due to link deformation. When the endpoint force are expressed in the base frame $\{C_0\}$, these small force and moment disappear as shown in

Fig. 7. Large noise appears in F_x due to the poor observability when using the bending and torsion strains to observe the axial force. To improve the measurement of F_x, the axial strain that associated with the internal axial force V_x may be required. The axial strains can be obtained using the same set of the strain gauges as used in the bending strain measurements but different bridge configurations (Gu, 2001*a*).

Table 1. Endpoint force under load 1.357 kg

Force	F_x	F_y	F_z	M_x	M_y	M_z
${}^0\mathbf{F}_a$	0	-13.30	0	-8.13	0	-1.17
${}^n\mathbf{F}_n$	1.17	-12.48	-1.20	-8.28	-0.30	-1.21
${}^0\mathbf{F}_n$	-0.54	-13.55	-0.40	-8.28	0.28	-1.19

In order to compare the detected endpoint forces ${}^n\mathbf{F}_n$ and ${}^0\mathbf{F}_n$ with the actual endpoint force. We obtained the actual endpoint force and moment according to the mass of the weight and the dimensions of the endpoint fixture and extension bar as shown in Fig. 4. The endpoint orientation of the flexible link has also been considered. For convenience, the actual force is denoted as ${}^0\mathbf{F}_a$.

Table 2. Endpoint force Under load 2.273 kg

Force	F_x	F_y	F_z	M_x	M_y	M_z
${}^0\mathbf{F}_a$	0	-22.28	0	-13.62	0	-1.96
${}^n\mathbf{F}_n$	2.64	-20.48	-2.21	-13.75	-0.85	-2.16
${}^0\mathbf{F}_n$	-0.54	-22.04	-0.55	-13.72	0.32	-2.02

Table 5 and Table 2 summarize the endpoint forces ${}^0\mathbf{F}_a$, ${}^n\mathbf{F}_n$ and ${}^0\mathbf{F}_n$ for the two loading weights. The units for the force and moment in the Tables are Newton (N) and Newton per meter (N/m) respectively. The actual endpoint force ${}^0\mathbf{F}_a$ is comparable to the detected endpoint force ${}^0\mathbf{F}_n$ since they are expressed in the same frame. From Table 5 and Table 2 we can see they are close to each other. The small errors are basically coming from the coordinate misalignment and measurement noise. However, the detected endpoint force ${}^n\mathbf{F}_n$ exhibits some difference to the actual endpoint force ${}^0\mathbf{F}_a$ because they are expressed in the different frames. This indicates that if a force sensor at end-effector is used for force control of flexible manipulator, it is still required to know the endpoint position and orientation of the flexible link when mapping the endpoint force from the endpoint frame $\{C_n\}$ to the base frame $\{C_0\}$. Otherwise, a misunderstanding of the endpoint force/moment will lead to an error in force control, especially for the flexible manipulator undergoing a large elastic deformation.

To illustrate the accuracy of the detection, the following equation is used to calculate the relative error for the endpoint force and moment:

$$e_r = \frac{actual\ \ force - detected\ \ force}{actual force} \times 100\% \quad (36)$$

Tatble 3 lists the relative errors for F_y, M_x and M_z under the two loading weights. It can be seen that the errors for the loading weight F_y are within 2 percent.

Table 3. Relative errors (in %)

Loading weight	$e_r - F_y$	$e_r - M_x$	$e_r - M_z$
1.357 kg	1.88	1.85	1.68
2.237 kg	1.08	0.95	3.06

6. CONCLUSION

We have demonstrated the use of flexible link as an endpoint position and force detection unit. The experimental results validate the proposed approach. Because this approach is dynamic-model free and involves only simple matrix calculations, it is easy to apply to a real system and does not require substantial computational resources. The position and force obtained in real-time can be directly used in kinematic transformation, static balance as well as hybrid position and force control of a flexible manipulator.

7. REFERENCES

Cannon, Jr, R. H. and E. Schmitz (1984). Initial experiment on the endpoint control of a flexible one-link robot. *International Journal of Robotics Research* **3**(3), 62–75.

Gu, Min (2001*a*). Determination of endpoint force and moment for flexible-link manipulators. Tech. Report CSA-TR-2001-0004. Space Technalogies, Canadian Space Agency.

Gu, Min (2001*b*). Kinematics of flexible manipulator: Modeling, simulation and tests. Tech. Report CSA-TR-2001-0003. Space Technologies, Canadian Space Agency.

Gu, Min and Jean-Claude Piedboeuf (2001). Determination of endpoint position and orientation of a flexible-link manipulator using strain gauges. *ASME Journal of Dynamic Systems, Measurement and Control*. (submitted).

Kim, Jin-Soo, Kuniaki Suzuki and Masaru Uchiyama (1996). Force control of a flexible manipulator based on measurement of link deflections. In: *Proceedings of the 1996 IEEE/RSJ International Conference on Intelligent Robots and Systems*. pp. 238–245. Part 1 (of 3).

Oakley, C. M. (1991). Experiments in Modeling and End-Point Control of Two-Link Flexible Manipulators. Phd thesis. Department of Mechanical Engineering, Stanford University, SUDAAR 603.

Piedboeuf, J-C. (1995). The Jacobian matrix for a flexible manipulator. *Journal of Robotic System* **12**(11), 709–726.

Piedboeuf, Jean-Claude and S. Miller (1994). Estimation of endpoint position and orientation of a flexible link using strain gauges. In: *Symposium on Robot Control*. Capri Italy. pp. 675–680.

Richter, K. and F. Pfeiffer (1991). A flexible link manipulator as a force measuring and controlling unit. In: *1991 IEEE International Conference on Robotics and Automation*. Sacramento, California. pp. 1214–1219.